AIMS Materials Science, 5(3): 479–493.
DOI: 10.3934/matersci.2018.3.479
Received: 15 March 2018
Accepted: 13 May 2018
Published: 21 May 2018

http://www.aimspress.com/journal/Materials

Research article

Properties and mechanisms of iodine doped of P3HT and P3HT/PCBM composites

Harold O. Lee III[1] and Sam-Shajing Sun[1,2,3,*]

[1] Center for Materials Research, Norfolk State University, 555 Park Avenue, Norfolk, VA 23504, USA
[2] PhD Program in Materials Science and Engineering, Norfolk State University, 555 Park Avenue, Norfolk, VA 23504, USA
[3] Department of Chemistry, Norfolk State University, 555 Park Avenue, Norfolk, VA 23504, USA

* **Correspondence:** Email: ssun@nsu.edu; Tel: +17578232993; Fax: +17578239054.

Abstract: Polymeric conjugated materials are very promising for developing future soft material based semiconductors, conductors, electronic and optoelectronic devices due to their inherent advantages such as lightweight, flexible shape, low-cost, ease of processability, ease of scalability, etc. Like their inorganic counterparts, the addition of certain minority molecules or dopants can significantly alter the electronic and optoelectronic properties of the host conjugated polymers or composites allowing tunablilty for a variety of electronic/optoelectronic applications. In this report, P3HT and P3HT:PCBM doped with various iodine concentrations or doping levels were systematically examined for potential electronic/optoelectronic properties. This study finds that a 5% mole ratio iodine doping resulting in a smallest P3HT inter-layer gap of about 6.5 nm in the P3HT edge-on main chain packing style as well as smallest exciton bandwidth and most intense or ordered H-style aggregates, which may account for an optimal electronic/optoelectronic performance of the 5% doped P3HT/PCBM device. The results and findings could be useful to understand and to guide the design and development of future generation high efficiency molecular or polymer based optoelectronic devices, including solar cells and photodetectors.

Keywords: P3HT; iodine doping; conductivity; aggregation

1. Introduction

Polymer based semiconductors and conductors exhibit inherent advantages such as lightweight, flexible shape, easily scalable, easily processable, low cost, and easily tunable [1]. Like inorganic semiconductors, polymeric semiconductors can also be doped with certain minority dopants to tune their electronic properties for specific applications. For inorganic semiconductors, doping is generally the replacement of a few crystalline atoms with atoms that have one more or less electron than the atoms in the host crystal [2]. For conducting polymers, dopant concentration can be as high as $10^{21}/cm^3$ which is orders of magnitude higher than in the typical inorganic case [2]. For instance, when polyacetylene was doped by iodine vapor, orders of magnitude increases in conductivity were observed [1,3–5]. Research on the doping of organic semiconductors has grown rapidly and the doped organic materials have been applied to a variety of electronic and optoelectronic systems such as organic/polymer solar cells and organic transistors [1]. Doping of π-conjugated polymers can turn them from insulating all the way to conducting materials, and doping has also been used to tune the optoelectronic properties of organic semiconductors [6,7]. Regio-regular poly(3-hexylthiophene-2,5-diyl) (P3HT) is one of the popular conjugated polymers for organic electronics and optoelectronics. P3HT's regio-regularity induced high solid-state packing order or crystallinity result in very good hole mobility (>1.0 cm^2/Vs) and strong visible light absorption down to 650 nm [8]. With the addition of a photo doping acceptor phenyl-C_{61}-butyric acid methyl ester (PCBM), a photo sensitive Donor/Acceptor bulk heterojunction composite form a prototypical polymer type solar cell. Due to a relatively low electrical conductivity of the P3HT:PCBM blend film, further chemical doping of the prototypical P3HT:PCBM blends with iodine has been shown to increase power conversion efficiencies which was attributed to conductivity increase [9]. While there are a number of reports on the chemical doping of P3HT, the iodine doping studies of P3HT:PCBM blends are rare. There are a number of recent reports on P3HT:PCBM composite doped with 2,3,5,6-Tetrafluoro-7,7,8,8-tetracyanoquinodimethane (F4-TCNQ) [10,11].

In recent years, significant progress has been made in understanding the relationship between the structure-property relationship in semiconducting polymers. But what has yet to be fully understood is how chemical doping is related to the electrical properties of these semiconducting polymers [12]. In classic inorganic systems, doping increases the charge carrier concentration as seen in Eq 1. Conductivity is defined as:

$$\sigma = eN\mu \tag{1}$$

where σ is the conductivity, e is the electric charge, N is the charge carrier density, and μ is the charge mobility. For chemically doped organic systems, electrical conductivity is not simply a function of charge carrier density, but it is also effected by the structural disorder that may occur during the doping process. To achieve p-type doping, dopant molecule lowest-occupied molecular orbital (LUMO) must be lower in energy than the highest-occupied molecular orbital (HOMO) than the host molecule. This energy offset can facilitate electron transfer from the host material (donor) to the dopant molecule (acceptor) and the scheme is shown in Figure 1.

Once this electron transfer occurs, positive charges are formed on the donor polymer chains causing localized structural distortion that could result in changings from benzoid to quinoid structure change in the conjugated backbone [13]. When chemical doping is done in solution, the charge transfer can lead to aggregation of the solution due to the formation of either charge-transfer

complexes or ion-pair formations [14]. These aggregates result in drastic changes in the overall thin film morphology and film properties and will be covered later on in this paper. This aggregation is similar to what was seen by Li et al. but is instead induced by chemical doping [15]. Another critical area to address is the optimum doping level for each dopant. Throughout literature, it has been shown that the optimum doping level is different depending on the p-type dopant. It is well known that in some organic semiconductors such as P3HT, the electrical conductivity versus dopant concentration is not a linear relationship. For example, when P3HT is doped with F4-TCNQ, as the dopant concentration is increased, a decrease in conductivity is observed at ultra-low and ultra-high doping levels followed by a linear and nonlinear increase at moderate doping levels, which is attributed to filling of electronic trap states [12]. In this report, we systematically studied the effects of iodine doping in P3HT:PCBM composite solutions and thin films. Our findings show that there is an optimum doping level for iodine doping of P3HT and we propose mechanisms of the interaction of iodine with P3HT:PCBM composites explaining how iodine induces morphological changes in these composite systems.

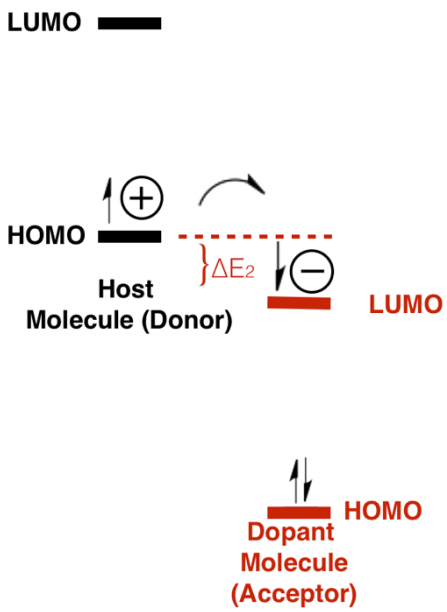

Figure 1. Schematic of chemical doping.

2. Materials and method

2.1. Sample preparation

P3HT (Product #: 698997) and PCBM (Product #: 684430) were used as received from Sigma-Aldrich without further purification. 1,2-dichlorobenzene (Product #: A13881) and iodine (Product #: A12278) were used as received from Alfa Aesar without further purification. A stock P3HT solution was made by dissolving 60 mg of P3HT into 4 mL of 1,2-dichlorobenzene resulting in a solution concentration of 15:1 mL of P3HT:1,2-dichlorobenzene. Solution doping was carried out by mole ratios of 1, 5, and 10% with respect to P3HT. 1, 5, and 10% mole ratio of iodine was weighed into individual vials. 1 mL aliquots of the stock solution were then placed into each vial

containing the different amounts of iodine. This resulted in solutions ranging from 0–10% iodine doped P3HT solutions. A stock P3HT:PCBM solution was made by dissolving 60 mg of P3HT and 60 mg of PCBM into 4 mL of 1,2-dichlorobenzene resulting in a solution concentration of 15:15:1 mL of P3HT:PCBM:1,2-dichlorobenzene. Solution doping was carried out by mole ratios of 1, 5, and 10% with respect to P3HT. 1, 5, and 10% mole ratio of iodine was weighed into individual vials. 1 mL aliquots of the stock solution were then placed into each vial containing the different amounts of iodine. This resulted in solutions ranging from 0–10% iodine doped P3HT:PCBM composites.

Thin films were prepared by spin coating previously prepared solutions onto plain glass slides. Glass slides were tripled sonicated in DI water, acetone, and isopropanol for five minutes each and then plasma cleaned in oxygen for 15 minutes. ITO coated glass slides for device fabrication were made by etching away ITO from the outside edges of the slide using 6 M hydrochloric acid leaving a strip of ITO in the center of the slide. The slides were then cleaned similar to plain glass slides minus the oxygen plasma cleaning. Solutions were then spin coated at 1000 rpm for 180 seconds. Thin films were then transferred in a vacuum oven and dried at 80 ℃ overnight (~17 hours) under −30 mmHg vacuum. It is important to note that films were dried individually, not all together, to prevent any cross contamination between doped samples. Devices were made by evaporating aluminum contacts through a shadow mask under 2×10^{-6} mbar vacuum in a thermal evaporator inside of an MBraun Glovebox. Device was constructed using the standard OPV device structure. Bottom electrode was Indium Tin Oxide and the top contact was aluminum. Figure 2 displays the resulting thin device fabricated from a top view and a layer by layer view. The entire thin film is irradiated by the solar simulator. Each device had an area of 0.25 cm^2.

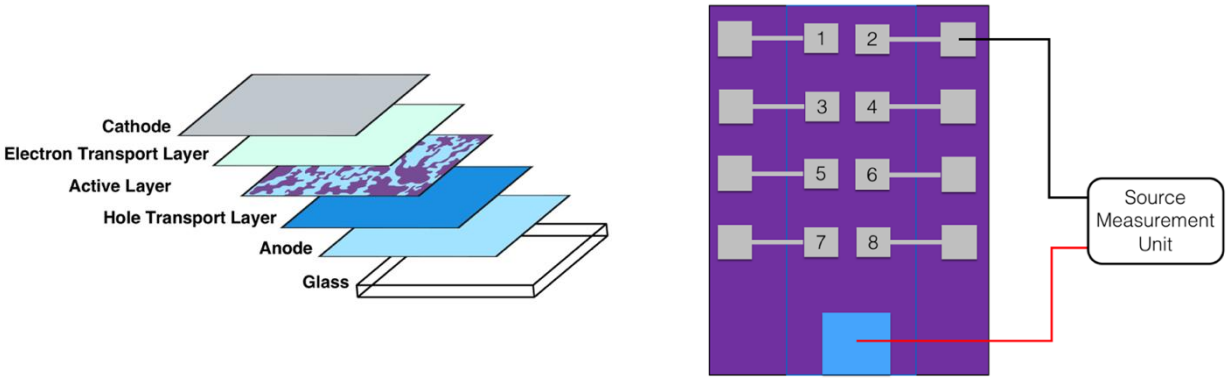

Figure 2. Schematic of final OPV devices side view (left) top view (right).

2.2. General instrumentation

Dynamic Light Scattering was conducted using a Microtrac Nanatrac Wave II. UV/Vis spectroscopy was conducted using a Perkin Elmer UV/Vis/NIR Spectrometer Lambda 1050 using the 60 mm InGaAs integrating sphere either in solution inside quartz vials or as thin films. Photoluminescence of the solutions were conducted using a Jobin-Yvon/Horiba Fluoromax-3 with an excitation wavelength of 518 nm for P3HT solutions and 508 nm for P3HT:PCBM solutions. Photoluminescence of the thin films were conducted at the National Renewable Energy Laboratory

using a custom setup. Atomic force microscopy (AFM) images were collected at the National Renewable Energy Laboratory on a Veeco Dimension Icon in tapping mode using a 300 kHz Silicon tip with a 40 N/m force constant, the scan area was set at 5 μm × 5 μm. AFM data analysis was conducted using a Nanoscope Analysis version 1.40 by Bruker. X-ray diffraction was conducted using a Rigaku X-ray Diffractometer using a Cu Kα source (λ = 1.5406 Å). Polymer film thicknesses were measured with a Dektak-6M profilometer. Thin film X-ray diffraction (XRD) studies were performed on a Rigaku D/Max-2200 TB X-ray Diffractometer (Cu Kα radiation, λ = 1.5406 Å).

2.3. Optoelectronic device fabrication and testing

Polymer solar cell devices were fabricated and tested inside a custom built MBraum inert gas glove box system coupled with a vacuum thermal deposition chamber (vacuum up to 1×10^{-7} mbar), a solar simulator (providing a one-Sun or 100 mW/cm^2, 1.5 AM simulated sunlight radiation), and a current-voltage source-measure-unit (Keithley SMU-237), and a data processing PC. Films were illuminated under 0.5 Sun (or 50 mW/cm^2, 1.5 AM simulated sunlight radiation) from an Oriel I kW Solar Simulator in an inert environment.

3. Results and discussion

In dichlorobenzene (DCB) solutions of iodine doped P3HT:PCBM composites in several glass vials, as the iodine concentration or doping level increased, the P3HT aggregation generated suspension particles become more obvious in the glass vials. For instance, a color change and a change in solution viscosity were observed as iodine concentration was increased. To better characterize this aggregation effect, dynamic light scattering (DLS) studies that are sensitive to aggregate or particle sizes in solution were measured. Figure 3 exhibits the DLS spectra of P3HT:PCBM dichlorobenzene (DCB) solutions at different iodine doping concentrations. It can be seen that the solution polymer aggregate particle sizes are around one nanometer in no iodine (a, top left) and 1% iodine doped P3HT:PCBM composites (b, top right), with the 1% iodine doped solution having a slightly broader particle size distribution than the undoped solution. However, the 5% iodine doped P3HT:PCBM composite solution yields a suspension particle size between 100–800 nm (c, lower left), while the 10% iodine doped solution yields a suspension particle size over 10000 nm (d, lower right). Interestingly, optical properties of 5% iodine doped solution appears unique to other doping levels (see Figures 4–6). Iodine doped P3HT:PCBM composite solutions displayed some similar traits as seen in F4-TCNQ doped P3HT:PCBM composite solutions in regards to aggregation in the solution phase. Lüssem et al. reports that at lower iodine doping concentrations, doped films of P3HT resemble the structure or morphology of undoped films of P3HT [16].

UV/Vis absorption and photoluminescence (PL) spectra were measured for iodine undoped and doped P3HT and P3HT:PCBM composites in dichlorobenzene (DCB) solution and thin film states. In the solution state, both pristine P3HT and P3HT:PCBM blend solutions were evaluated. Figures 4 and 5 exhibit the UV/Vis and PL spectras of pristine P3HT dichlorobenzene (DCB) solutions with various concentrations of iodine. In the UV/Vis, as the concentration or doping levels of iodine increase, the main absorption peak at about 465 nm decreases while an absorption shoulder peak at longer wavelength of about 610 nm increases. This 610 nm shoulder peak is believed to be due to

P3HT H-type aggregate formation as a result of iodine doping level at or above 5% as can be seen in the thin films as well. It is interesting to note that 5% doping results in slightly higher 610 nm should peak then the 10% doped one. In the PL spectra shown in Figure 7, the PL intensity quenches as the iodine concentration increases, and the PL quenching can be attributed to iodine doping induced charge separation between P3HT and the iodine that suppresses the exciton PL emission.

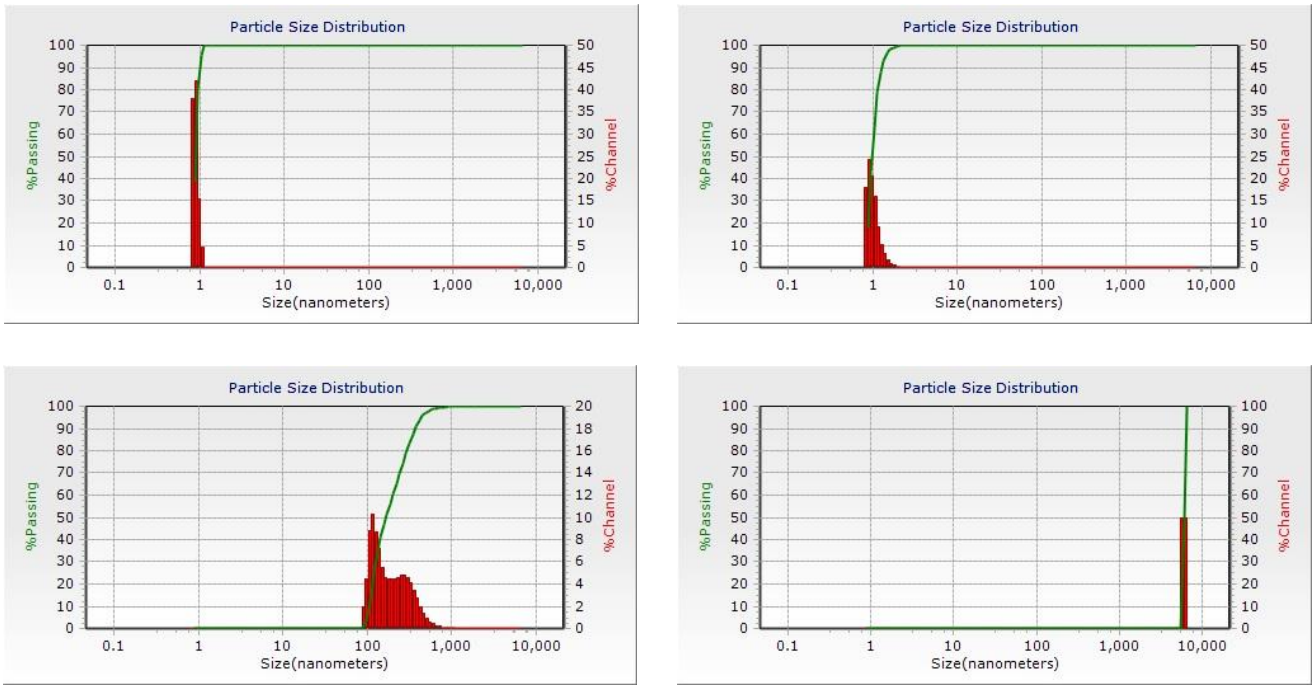

Figure 3. Dynamic Light Scattering (DLS) spectra of P3HT:PCBM in dichlorobenzene (DCB) solutions doped by iodine at (a) 0% shown in top left; (b) 1% shown in top right; (c) 5% shown in bottom left; (d) 10% bottom right.

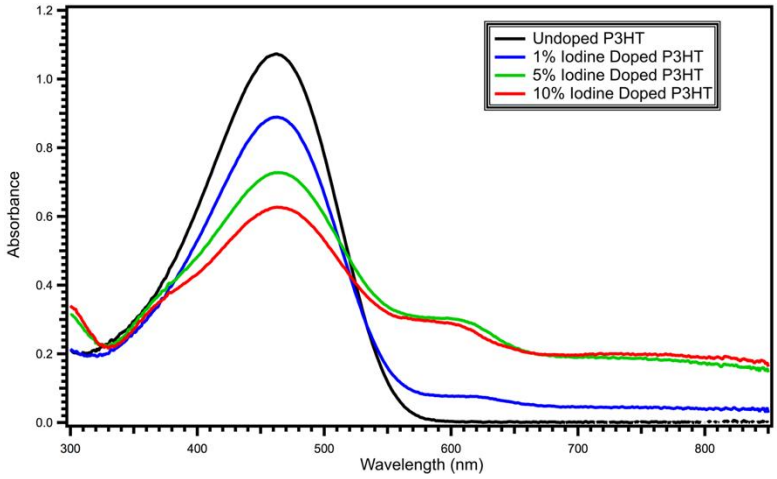

Figure 4. UV/Vis spectra of P3HT dichlorobenzene (DCB) solutions with various iodine concentrations.

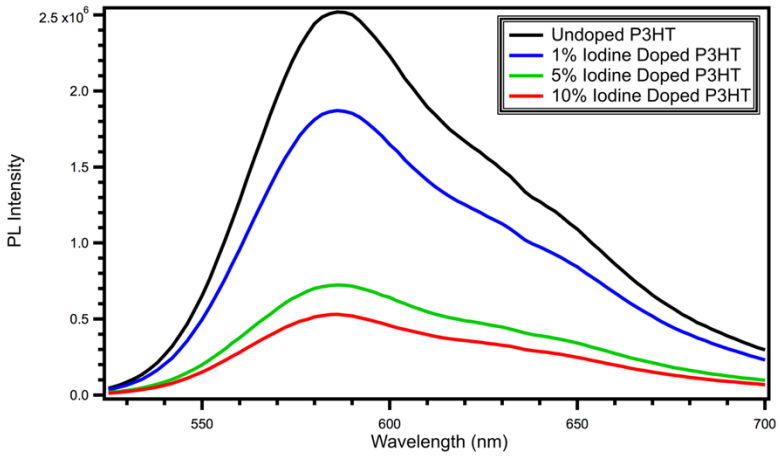

Figure 5. PL spectra of P3HT dichlorobenzene (DCB) solutions with various iodine concentrations.

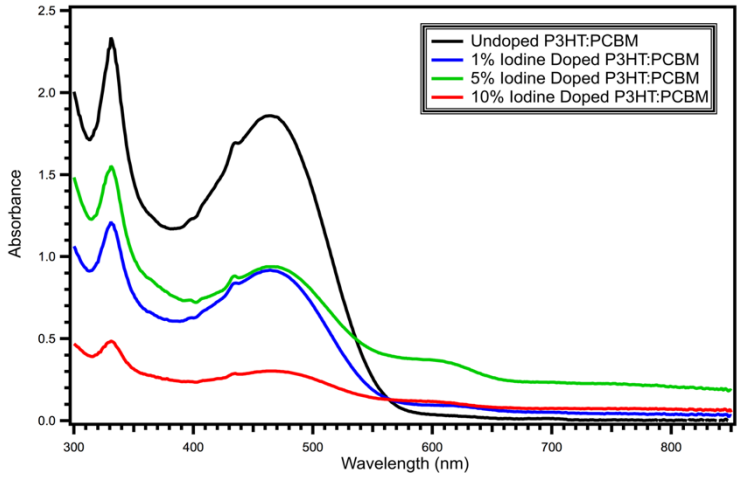

Figure 6. UV/Vis spectra of P3HT:PCBM dichlorobenzene (DCB) solutions with various iodine concentrations.

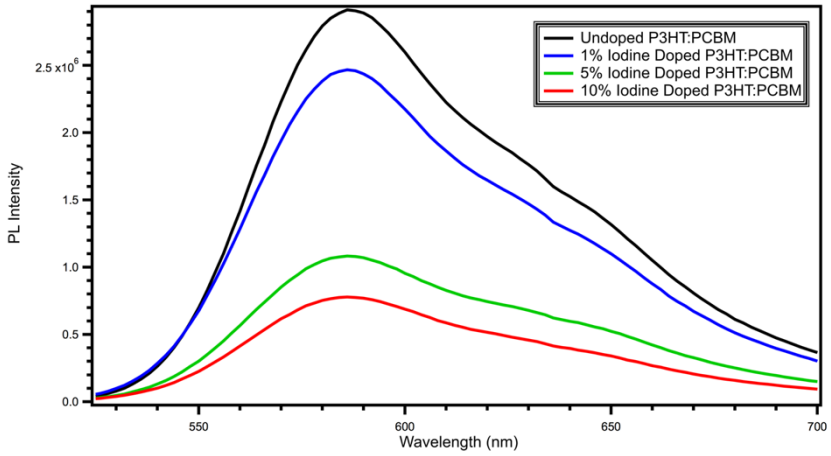

Figure 7. PL spectra of P3HT:PCBM dichlorobenzene (DCB) solutions with various iodine concentrations.

Figures 6 and 7 exhibit the UV/Vis and PL spectras of P3HT:PCBM composite solutions with various concentrations of iodine doping. Again, in the UV/Vis the main absorption peak at around 465 nm decreases and an absorption shoulder peak at about 610 nm increases. Notably, the 5% iodine doped shoulder peak at 610 nm was much higher than both the 1% and 10% iodine doped ones, indicating something unique in the 5% iodine doped P3HT:PCBM as compared to other doping levels. Again, as shown in Figure 7, PL intensity quenches as the iodine concentration increases.

The UV/Vis and PL studies of P3HT:PCBM solid thin films were also carried out with varying iodine doping levels. In the UV-Vis thin film samples as shown in Figure 8, four distinct peaks are shown. The peak at around 335 nm is attributed to the PCBM. It is believed that the peak around 515 nm corresponds to intra-chain or main chain π-conjugated electron excitations, and that this peaks' intensity is heavily influenced by the film thickness [8]. The peaks around 560 and 610 nm are believed due to inter-chain π–π stacking or polymer solid state H-type aggregates packing, where the Frenkel type inter-chain exciton bandwidth *W* can be estimated using the 560 nm and 610 nm peaks and shown in Figure 9 [8]. The film thickness was also increased as a function of iodine concentration at the same thin film processing condition due to an iodine doping induced increase in solution viscosity and aggregation (Additional data are listed in Figure S1 of the Supporting Information).

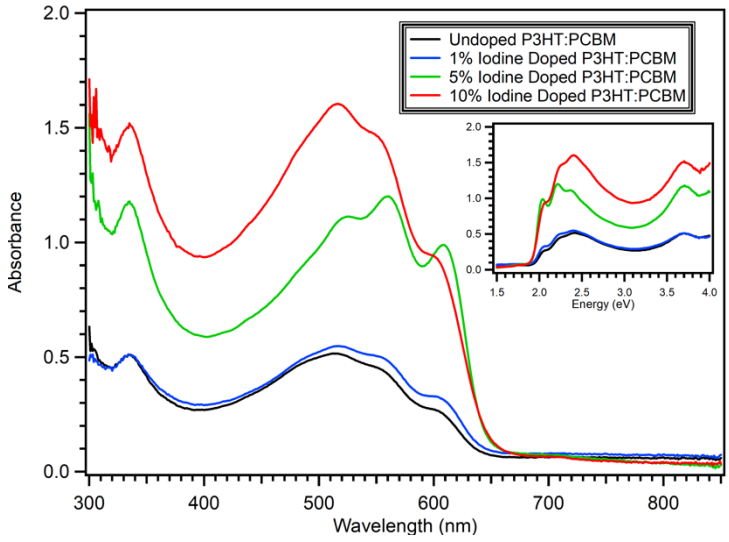

Figure 8. UV/Vis spectra of P3HT:PCBM thin films at various iodine doping levels.

Several research groups have reported that increased absorption at shoulder peaks 560 nm and 610 nm are directly related to the increased solid-state H-type aggregates packing order [8,17,18]. Baghgar et al. mentioned P3HT aggregates can adopt either J- or H-aggregate configurations which favor intra-chain and inter-chain order respectively [19]. H-aggregates exhibits blue-shift of absorption peak as compared to non-aggregates due to higher excited state energies, while J-aggregates exhibits red-shift absorption peak as compared to non-aggregates due to lower excited states energies [19]. UV/Vis and PL techniques should be run in conjunction with each other because the entire matrix may absorb but only the most ordered segments may be obvious in PL [11,20,21]. In the thin film PL spectra shown in Figure 10, we see blue shift in the main emission peak at iodine concentrations greater than 5%, but the shoulder peak remains at a relatively similar position for all

films. It is important to know that the 0–0 transition is the lowest energy absorption feature [20]. UV/Vis and PL are characterization tools that should be run in conjunction with each other because the entire matrix absorbs but only the most ordered segments may be obvious in PL [10,20,22]. Also, note that in the UV/Vis, there are three distinct absorption peaks while in the PL there are only two. This confirms what other research groups have observed, i.e., only the most ordered segments could be characterized via PL. One additional parameter to characterize P3HT thin film aggregates is their exciton bandwidth *W* as estimated from the two vibronic shoulder peaks of 560 nm and 610 nm and as shown in Figure 9 [23]. It is interesting to note that 5% iodine doping corresponds to the smallest exciton bandwidth of about 0.05 eV. Typically, the exciton bandwidth *W* here reflects the dispersive or amorphous nature of H-type aggregates, i.e., smallest bandwidth corresponds least dispersive or most ordered H-aggregates [23]. Also, it is well known that the exciton bandwidth is inversely proportional to the charge transport properties of the material meaning lower *W* leads to higher conductivities [14].

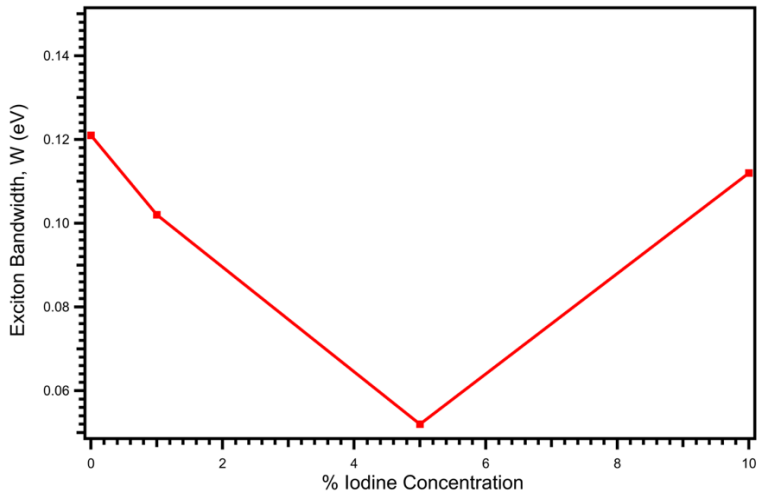

Figure 9. Exciton bandwidth vs. iodine doping levels.

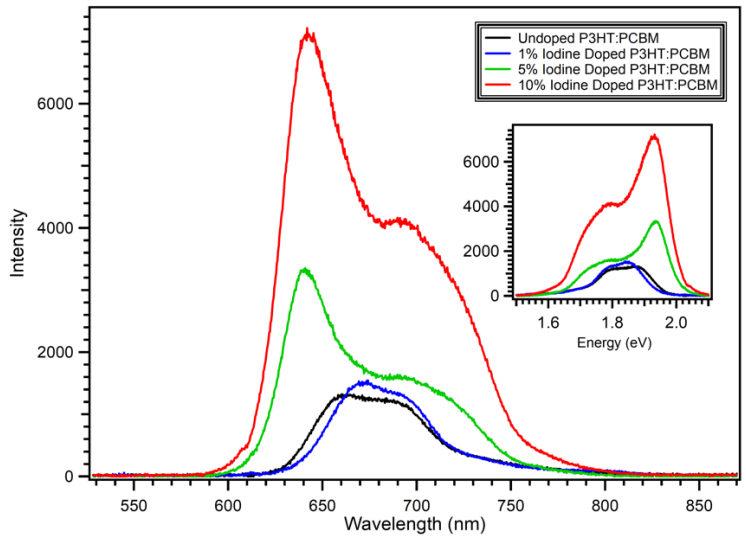

Figure 10. PL spectra of P3HT:PCBM thin films with various iodine doping levels.

X-ray diffraction (XRD) was also used to investigate the crystallinity and solid state packing of different iodine doped polymer samples. Figure 11 displays the XRD spectra of P3HT:PCBM thin films on glass with various iodine doping levels. The first peak at around $2\theta = 5.48°$ corresponds to the (100) direction plain which is the alkyl side chain direction when the P3HT is in the most popular edge-on packing style. At 5% iodine, the peak intensity at around $2\theta = 5.48°$ is greatest representing the greatest degree of order or crystallinity similar to the results Kim et al. observed [11]. Figure 12 shows the correlation between the XRD peak intensity versus iodine doping levels.

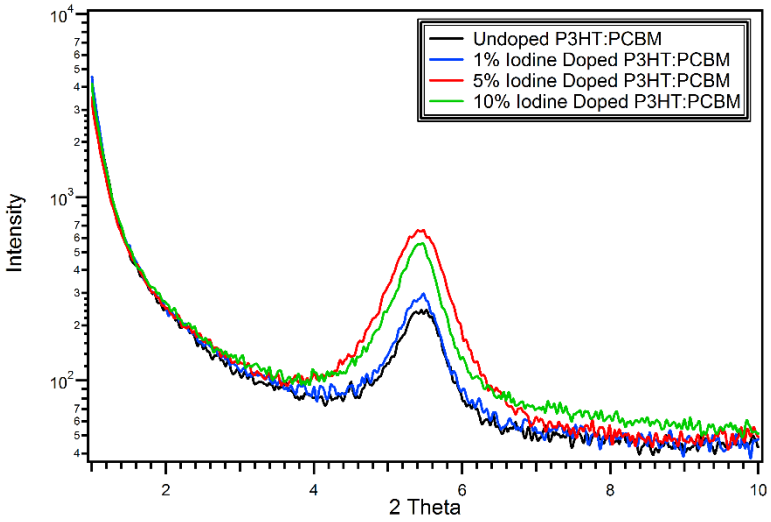

Figure 11. XRD spectra of P3HT:PCBM thin films with various iodine doping levels.

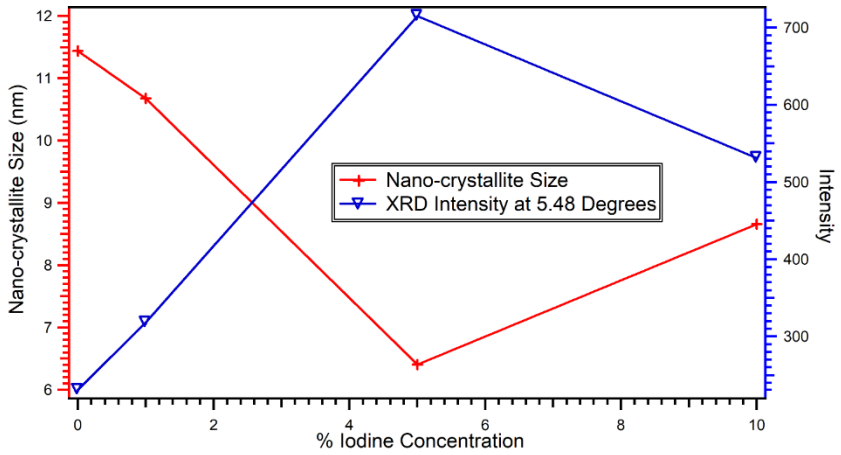

Figure 12. XRD 100 plain peak intensity (at $2\theta = 5.48$) versus iodine doping levels (blue) and the P3HT Edge-on vertical (Z direction) inter-layer spacing (nanocrystallite sizes) versus iodine doping levels (red).

As Figure 12 shows, at 5% iodine, the calculated nano-crystallite size (corresponding to the P3HT edge-on inter-layer gap) was smallest. Since the peak for the (100) direction was used, this nano-crystallite size corresponds to the P3HT edge-on style packing inter-layer gap or the alkyl side chain interdigitation. This is in good agreement with the results obtained by Winokur et al. [9].

Overall, at 5% iodine doping level, we observed the smallest exciton bandwidth, the highest XRD diffraction peak intensity, along with the smallest inter-layer gap of P3HT edge-on style packing. The equations used for these calculations are listed in the supporting information.

Atomic Force Microscopy (AFM) was measured to study surface morphology of the thin films. The AFM images are shown in the supporting information. Using the average and RMS surface roughness values obtained from the AFM, the surface roughness was plotted against the iodine doping levels as shown in Figure 13. Again, at 5% iodine doping level, thin films are smoothest in comparison to other doping levels.

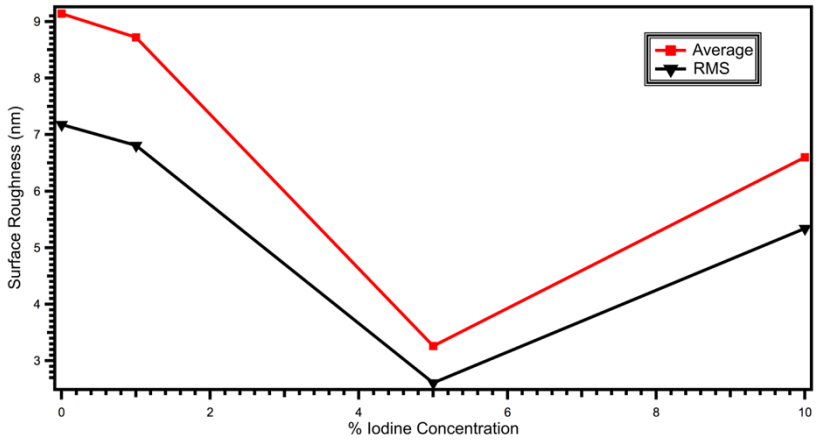

Figure 13. Average RMS surface roughness of P3HT:PCBM thin films with various iodine doping levels.

Finally, optoelectronic devices were fabricated to evaluate the iodine doping effects on device performance. Figure 14 displays the conductivity of P3HT/PCBM composite thin films with various iodine doping levels. Again, 5% iodine doped samples exhibit highest conductivity versus other doping levels. Figure 15 displays IV curves comparing undoped and 5% iodine doped samples, and the doped one exhibit better performance than the undoped one confirming an earlier report [9].

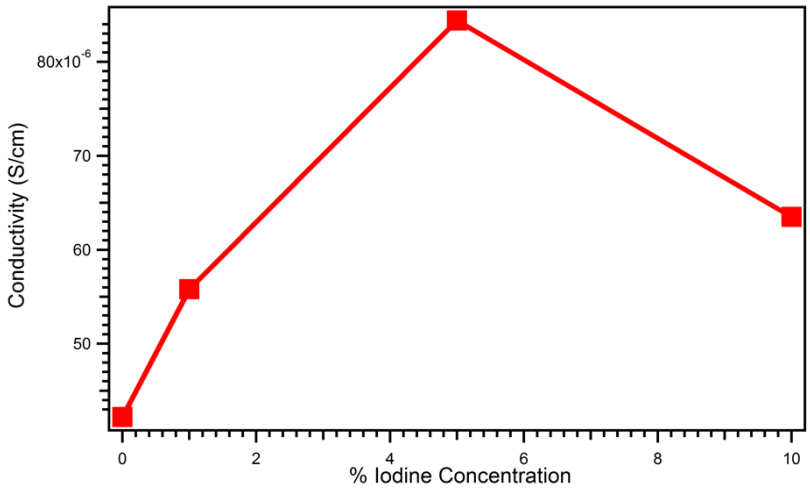

Figure 14. Electrical conductivity of P3HT/PCBM films versus iodine doping levels.

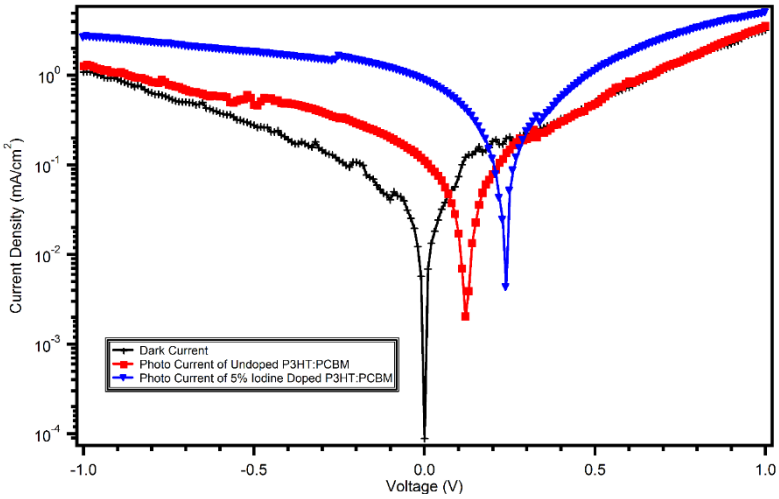

Figure 15. J-V curves of undoped and 5% iodine doped P3HT:PCBM solar cells under dark and illuminated conditions.

From our experimental results, it is evident that the iodine induces some structural changes in the polymer main chain. The XRD indicates that the interdigitation between polymer chains increases as seen in the decrease in interspacing distances in the 100 direction of edge-on packed P3HT, which is the alkyl side chain direction. This agrees with Winokur et al. in which then observed the same phenomena. Tashiro et al. mention that the polythiophene skeletal chain has a direct interaction with the iodine ions, meaning that they should be in close proximity with each other [24]. With this in mind, we propose another way in which iodine could facilitate this increased interdigitation.

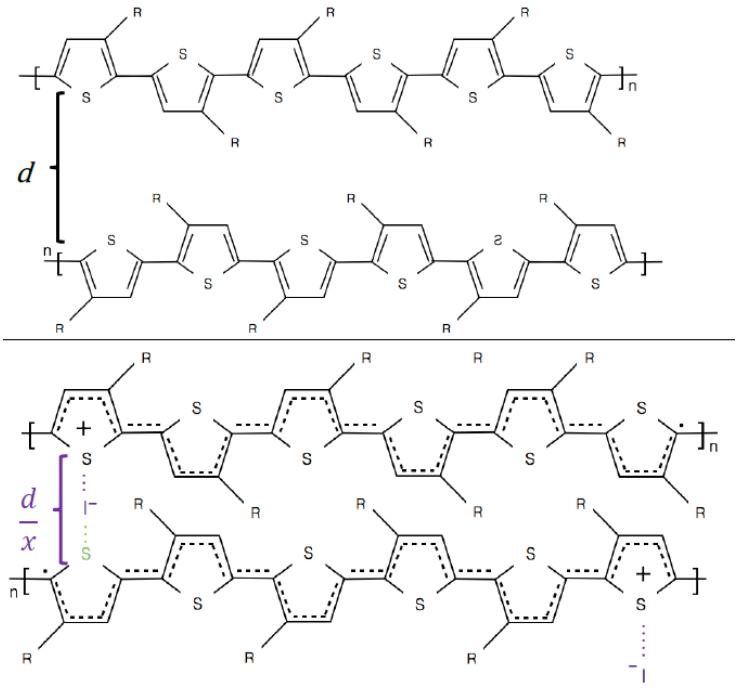

Figure 16. Schematic of undoped (top) and doped (bottom) P3HT in the proposed mechanism of iodine doping effects on structure.

Figure 16 presents the structures undoped and doped P3HT. We propose that the iodine ions can potentially interact with two sulfur atoms within neighboring thiophene rings. With iodine's high polarizability, the coulombic attraction with two thiophene rings brings them closer to the iodine ion resulting in the two chains seemingly becoming more interdigitated.

4. Conclusions

In conclusion, UV/Vis spectroscopy, photoluminescence quenching, and solution dynamic light scattering studies reveals that iodine doping can result in P3HT main chain aggregations even in solution. In the solid state thin films, UV/Vis spectroscopy, photoluminescence, atomic force microscopy, and X-ray diffraction reveals that iodine doping increases surface smoothness and H-type aggregate crystallinity in P3HT:PCBM thin films. The smallest exciton bandwidth and smallest inter-layer gap of about 6.5 nm on P3HT edge-on film packing style was observed on the 5% iodine doped P3HT:PCBM composite thin films which correspond to P3HT highest order H-type aggregates formation, and this may account for an optimal solar cell performance at 5% iodine doping level reported earlier [25]. This work could be helpful to understand the mechanisms of chemical doping of conjugated polymers at the molecular level and their correlations to materials bulk electronic and optoelectronic properties for variety applications.

Acknowledgments

This material is based upon work supported, in part, by research and/or educational grant awards from a number of agencies including the Department of Defense (Award # W911NF-15-1-0422) and the National Science Foundation (NSF Award # HRD-1547771).

Conflict of interest

All authors declare no conflicts of interest in this paper.

References

1. Sun SS, Dalton LR (2016) *Introduction to Organic Electronic and Optoelectronic Materials and Devices*, 2 Eds, Boca Raton: CRC Press/Taylor & Francis.
2. Li Y, Hou J (2016) Major Classes of Conjugated Polymers and Synthetic Strategies, In: Sun SS, Dalton LR, *Introduction to Organic Electronic and Optoelectronic Materials and Devices*, 2 Eds, Boca Raton: CRC Press/Taylor & Francis, 190–194.
3. Chiang CK, Fincher Jr CR, Park YW, et al. (1977) Electrical Conductivity in Doped Polyacetylene. *Phys Rev Lett* 39: 1098–1101.
4. Sun SS (2016) Basic Electronic Structures and Charge Carrier Generation in Organic Optoelectronic Materials, In: Sun SS, Dalton LR, *Introduction to Organic Electronic and Optoelectronic Materials and Devices*, 2 Eds, Boca Raton: CRC Press/Taylor & Francis, 77–87.
5. Sun SS, Sariciftci NS (2005) *Organic Photovoltaics: Mechanisms, Materials, and Devices*, Boca Raton: CRC Press/Taylor & Francis.

6. Komarudin D, Morita A, Osakada K, et al. (1988) Iodine Doping of Poly(thiophene-2,5-diyl) and poly(3-Alkylthiophene-2,5-Diyl)s in Aqueous Media. *Polym J* 30: 860–862.
7. Tian P, Tang L, Xiang J, et al. (2016) Solution Processable High-Performance Infrared Organic Photodetector by Iodine Doping. *RSC Adv* 6: 45166–45171.
8. Li G, Shrotriya V, Huang JS, et al. (2006) Polymer Self-Organization Enhances Photovoltaic Efficiency. *SPIE Newsroom*. Available from: http://spie.org/newsroom/0147-polymer-self-organization-enhances-photovoltaic-efficiency?ArticleID=x8808.
9. Winokur MJ, Wamsley P, Moulton J, et al. (1991) Structural evolution in iodine-doped poly(3-alkylthiophenes). *Macromolecules* 24: 3812–3815.
10. Gao J, Niles ET, Grey JK (2013) Aggregates Promote Efficient Charge Transfer Doping of Poly(3-Hexylthiophene). *J Phys Chem Lett* 4: 2953–2957.
11. Gao J, Roehling JD, Li Y, et al. (2013) The Effect of 2,3,5,6-Tetrafluoro-7,7,8,8-Tetracyanoquinodimethane Charge Transfer Dopants on the Conformation and Aggregation of poly(3-Hexylthiophene). *J Mater Chem C* 1: 5638–5646.
12. Lim E, Peterson KA, Su GM, et al. (2018) Thermoelectric Properties of Poly(3-hexylthiophene) (P3HT) Doped with 2,3,5,6-Tetrafluoro-7,7,8,8-tetracyanoquinodimethane (F4TCNQ) by Vapor-Phase Infiltration. *Chem Mater* 30: 998–1010.
13. Enengl C, Enengl S, Pluczyk S, et al. (2016) Doping-Induced Absorption Bands in P3HT:Polarons and Bipolarons. *ChemPhysChem* 17: 3836–3844.
14. Salzmann I, Heimel G, Oehzelt M, et al. (2016) Molecular Electrical Doping of Organic Semiconductors: Fundamental Mechanisms and Emerging Dopant Design Rules. *Accounts Chem Res* 49: 370–378.
15. Li P, Chen LJ, Pan J, et al. (2014) Dispersion of P3HT gelation and its influence on the performance of bulk heterojunction organic solar cells based on P3HT:PCBM. *Sol Energ Mat Sol C* 125: 96–101.
16. Lüssem B, Riede M, Leo K (2013) Doping of Organic Semiconductors. *Phys Status Solidi A* 210: 9–43.
17. Chen TA, Wu X, Rieke RD (1995) Regiocontrolled Synthesis of Poly(3-Alkylthiophenes) Mediated by Rieke Zinc: Their Characterization and Solid-State Properties. *J Am Chem Soc* 117: 233–244.
18. Liao HC, Hsu CP, Wu MC, et al. (2013) Conjugated Polymer/nanoparticles Nanocomposites for High Efficient and Real-Time Volatile Organic Compounds Sensors. *Anal Chem* 85: 9305–9311.
19. Baghgar M, Barnes MD (2015) Work Function Modification in P3HT H/J Aggregate Nanostructures Revealed by Kelvin Probe Force Microscopy and Photoluminescence Imaging. *ACS Nano* 9: 7105–7112.
20. Brown PJ, Thomas DS, Köhler A, et al. (2003) Effect of Interchain Interactions on the Absorption and Emission of poly(3-Hexylthiophene). *Phys Rev B* 67: 64203.
21. Endrodi B, Mellár J, Gingl Z, et al. (2015) Molecular and Supramolecular Parameters Dictating the Thermoelectric Performance of Conducting Polymers: A Case Study Using poly(3-Alkylthiophene)s. *J Phys Chem C* 119: 8472–8479.
22. Ehrenreich P, Birkhold ST, Zimmermann E, et al. (2016) H-Aggregate Analysis of P3HT Thin Films-Capability and Limitation of Photoluminescence and UV/Vis Spectroscopy. *Sci Rep* 6: 32434.

23. Clark J, Chang JF, Spano FC, et al. (2009) Determining exciton bandwidth and film microstructure in polythiophene films using linear absorption spectroscopy. *Appl Phys Lett* 94: 163306.
24. Tashiro K, Kobayashi M, Kawai T, et al. (1997) Crystal structural change in poly(3-alkyl thiophene)s induced by iodine doping as studied by an organized combination of X-ray diffraction, Infrared/Raman spectroscopy and computer simulation techniques. *Polymer* 38: 2867–2879.
25. Zhuo Z, Zhang F, Wang J, et al. (2011) Efficiency Improvement of Polymer Solar Cells by Iodine Doping. *Solid State Electron* 63: 83–88.

AIMS Press